Electronic Supporting Information

Mechanistic insight into electrocatalytic glyoxal reduction on copper and its relation to CO$_2$ reduction

Andreas M. Reichert,[‡,a] Oriol Piqué,[‡,b] Walter A. Parada,[a]

Ioannis Katsounaros*,[a] and Federico Calle-Vallejo, *,[b,c,d]

[a] Helmholtz Institute Erlangen-Nürnberg for Renewable Energy (IEK-11), Forschungszentrum Jülich GmbH, Cauerstr. 1, 91058 Erlangen, Germany.

[b] Department of Materials Science and Chemical Physics & Institute of Theoretical and Computational Chemistry (IQTC), University of Barcelona, Martí i Franquès 1, 08028 Barcelona, Spain.

[c] Nano-Bio Spectroscopy Group and European Theoretical Spectroscopy Facility (ETSF), Department of Polymers and Advanced Materials: Physics, Chemistry and Technology, University of the Basque Country UPV/EHU, Avenida Tolosa 72, 20018 San Sebastián, Spain.

[d] IKERBASQUE, Basque Foundation for Science, Plaza de Euskadi 5, 48009 Bilbao, Spain.

Table of Contents

S1. Electrochemical cell

Figure S1 shows the most important components of the electrochemical cell that was used in this study.
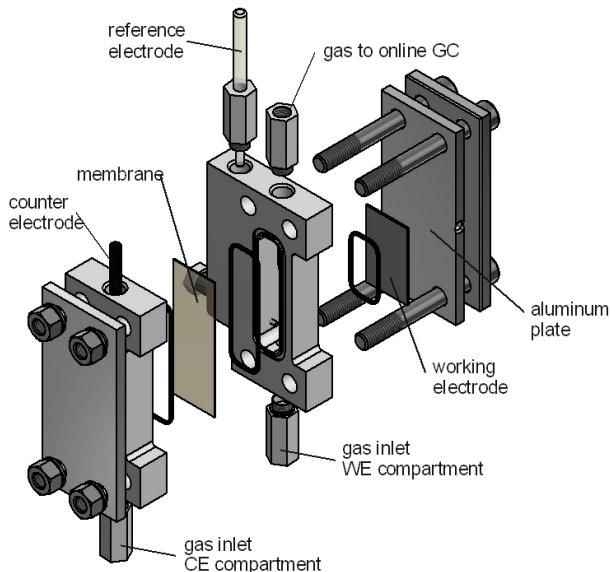

Figure S1. Electrochemical cell for steady-state electrolysis.

S2. Calculations of partial current density, faradaic efficiency and yield (carbon balance)

We considered the following electrochemical half-reactions:

Glyoxal to ethanol: $C_2H_2O_2 + 5H_2O + 6e^- \rightleftarrows C_2H_5OH + 6OH^-$
Glyoxal to acetaldehyde: $C_2H_2O_2 + 3H_2O + 4e^- \rightleftarrows CH_3CHO + 4OH^-$
Glyoxal to ethylene glycol: $C_2H_2O_2 + 4H_2O + 4e^- \rightleftarrows (CH_2OH)_2 + 4OH^-$
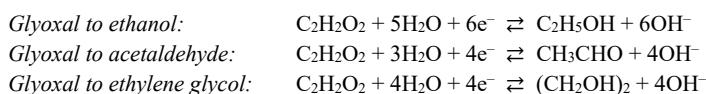
The partial current density for the formation of a certain product, j_i (in A cm^{-2}), was calculated using Faraday's law (Equation S1):

$$j_i = \frac{n_i z_i F}{At} \quad (S1)$$

where:
n_i is the moles of product i detected in the electrolyte in the end of electrolysis;
z_i is the number of electrons exchanged for the formation of one molecule in the corresponding reaction;
F is the faraday constant (96,485 A s mol^{-1});
A is the geometric electrode area (1 cm^2);
t is the duration of electrolysis (2,400 s).

The faradaic efficiency for a certain product, FE$_i$ (in %), was calculated by equation S2:

$$FE_i = \frac{j_i}{j_{total}} \cdot 100 \quad (S2)$$

where:
j_{total} is the average current density recorded during the electrolysis experiment.

2

To determine the percentage of unreacted glyoxal, U (in %) and the yield for each product (Y_i, in %), the equations S3 and S4 were used:

$$U = \frac{(n_o - n_{40})}{n_o} \cdot 100 \qquad \text{(S3)}$$

$$Y_i = \frac{n_i}{n_o} \cdot 100 \qquad \text{(S4)}$$

where:

n_o is the moles of glyoxal prior to electrolysis (1.8 10^{-3} mol for the 9 mL catholyte);

n_{40} is the moles of gloyxal found in the electrolyte after 40 min of electrolysis.

S3. Gas and liquid phase corrections

The free energies of gas-phase molecules were approximated as: $G \approx E_{DFT} + ZPE - TS$. The ZPE values were obtained from vibrational frequency analyses and the TS values were extracted from thermodynamic tables at 298.15 K and 1 atm.[1] Using a method described elsewhere,[2] we applied corrections to the total energies of the gas phase, denoted GC. Moreover, we added liquid-phase corrections based on the entropy differences between liquid and gas phases as described elsewhere,[3] denoted LC. The values used for all the liquids and gases in this study are listed in Table S1.

Table S1. Zero-point energy, entropy contributions, gas- and liquid-phase corrections to the free energies of molecules featured in this work. All values are in eV.

Molecule	ZPE	TS	GC	LC
H_2	0.27	0.40	0.00	0.00
H_2O	0.57	0.58	0.00	-0.09
O_2	0.10	0.63	-0.46	0.00
Glyoxal	0.97	0.84	-0.14	0.00
Acetaldehyde	1.46	0.82	-0.02	0.06
Ethanol	2.11	0.87	0.03	-0.07
Ethylene glycol	2.24	0.94	0.14	-0.27

S4. Contributions to the free energies of solvent-adsorbate interactions

Water-adsorbate interactions deemed "solvation" corrections (E_{sol} in $G \approx E_{DFT} + ZPE - TS + E_{sol}$) were computed on Cu(111) using an iterative method described elsewhere.[4] The specific values are listed in Table S2.

Table S2. Stabilization (in eV) provided by water-adsorbate interactions to the adsorption energies.

Adsorbate	Solvation correction
*CHOCHO	-0.36
*CHOHCHO	-0.31
*CH₂OCHO	0.00

*CHCHO	-0.34
*CHOHCHOH	-0.28
*CH₂OHCHO	-0.39
*CHOHCH₂O	-0.30
*CHOHCH₂OH	-0.19

S5. Free energies and active sites

The ZPE, TS$_{vib}$, solvation energy (E$_{sol}$), and the corresponding ΔG values obtained for the different adsorbates on the different model surfaces featured in the electroreduction of glyoxal to ethylene glycol are shown in Table S3. Note that gas-phase glyoxal and the clean surfaces were used as a reference for the free energies of the intermediates.

Table S3. Free energies of adsorption and their contributions (in eV) for the adsorbed species involved in the most favorable pathway of the electrochemical reduction of glyoxal to ethylene glycol.

Cu(111)	ZPE	TS	E$_{sol}$	ΔG
*CHOCHO	1.02	0.25	-0.36	-0.56
*CHOHCHO	1.32	0.31	-0.31	-0.48
*CHOHCHOH	1.61	0.52	-0.28	-0.45
*CHOHCH₂OH	1.93	0.38	-0.19	-0.11
Cu(100)	**ZPE**	**TS**	**E$_{sol}$**	**ΔG**
*CHOCHO	1.03	0.22	-0.36	-1.09
*CHOHCHO	1.32	0.29	-0.31	-0.89
*CHOHCHOH	1.62	0.39	-0.28	-0.50
*CHOHCH₂OH	1.94	0.39	-0.19	-0.36
Cu(211)	**ZPE**	**TS**	**E$_{sol}$**	**ΔG**
*CHOCHO	1.02	0.29	-0.36	-1.32
*CHOHCHO	1.34	0.30	-0.31	-1.07
*CHOHCHOH	1.61	0.36	-0.28	-0.75
*CHOHCH2OH	1.94	0.35	-0.19	-0.67
4AD@Cu(100)	**ZPE**	**TS**	**E$_{sol}$**	**ΔG**
*CHOCHO	1.04	0.22	-0.36	-1.56
*CHOHCHO	1.34	0.27	-0.31	-1.40
*CHOHCHOH	1.61	0.42	-0.28	-0.76
*CHOHCH2OH	1.95	0.37	-0.19	-0.73
4AD@Cu(111)	**ZPE**	**TS**	**E$_{sol}$**	**ΔG**
*CHOCHO	1.03	0.22	-0.36	-1.80
*CHOHCHO	1.34	0.26	-0.31	-1.44
*CHOHCHOH	1.62	0.32	-0.28	-0.79

*CHOHCH2OH	1.95	0.42	-0.19	-0.86

The ZPE, TS$_{vib}$, solvation energy (E$_{sol}$), and the corresponding ΔG values obtained for the different adsorbates on the different model surfaces featured in the electroreduction of glyoxal to ethanol are shown in Table S4. From *CH$_2$CHO on the values are extracted from previous works[5,6] and adapted because the gas-phase references are different. Here, gas-phase glyoxal and the clean surfaces were used as a reference for the free energies of the intermediates.

Table S4. Free energies of adsorption and their contributions (in eV) for the species involved in the electrochemical reduction of glyoxal to ethanol. Values extracted and adapted from previous works[5,6] are shown in *italics*. Liquid acetaldehyde was used when it was more stable than its adsorbed counterpart.

Cu(111)	**ZPE**	**TS**	**E$_{sol}$**	**ΔG**
*CHOCHO	1.02	0.25	-0.36	-0.56
*CHOHCHO	1.32	0.31	-0.31	-0.48
*CHCHO	0.90	0.19	-0.34	-1.29
*CH$_2$CHO	-	-	-	*-1.66*
CH$_3$CHO$_{(l)}$	-	-	-	*-1.81*
*CH$_3$CH$_2$O	-	-	-	*-0.99*
Cu(100)	**ZPE**	**TS**	**E$_{sol}$**	**ΔG**
*CHOCHO	1.03	0.22	-0.36	-1.09
*CHOHCHO	1.32	0.29	-0.31	-0.89
*CHCHO	0.91	0.17	-0.34	-1.64
*CH$_2$CHO	-	-	-	*-1.93*
CH$_3$CHO$_{(l)}$	-	-	-	*-1.81*
*CH$_3$CH$_2$O	-	-	-	*-1.36*
Cu(211)	**ZPE**	**TS**	**E$_{sol}$**	**ΔG**
*CHOCHO	1.02	0.29	-0.36	-1.32
*CHOHCHO	1.34	0.30	-0.31	-1.07
*CHCHO	0.91	0.17	-0.34	-1.65
*CH$_2$CHO	-	-	-	*-2.09*
*CH$_3$CHO	-	-	-	*-2.01*
*CH$_3$CH$_2$O	-	-	-	*-1.54*
4AD@Cu(100)	**ZPE**	**TS**	**E$_{sol}$**	**ΔG**
*CHOCHO	1.04	0.22	-0.36	-1.56
*CHOHCHO	1.34	0.27	-0.31	-1.40
*CHCHO	0.91	0.17	-0.34	-2.03
*CH$_2$CHO	-	-	-	*-2.24*
*CH$_3$CHO	-	-	-	*-2.03*
*CH$_3$CH$_2$O	-	-	-	*-1.86*
4AD@Cu(111)	**ZPE**	**TS**	**E$_{sol}$**	**ΔG**
*CHOCHO	1.03	0.22	-0.36	-1.80
*CHOHCHO	1.34	0.26	-0.31	-1.44
*CHCHO	0.91	0.16	-0.34	-2.03

*CH₂CHO	-	-	-	-2.47
*CH₃CHO	-	-	-	-2.11
*CH₃CH₂O	-	-	-	-2.05

Figure S2 shows the top views of the five active sites under study. The generalized coordination number $\overline{CN}(i)$ is arithmetically calculated as shown in Equation S5 for a given surface site "i":

$$\overline{CN}(i) = \sum_{j=1}^{n_i} \frac{cn(j)}{cn_{max}} \quad (S5)$$
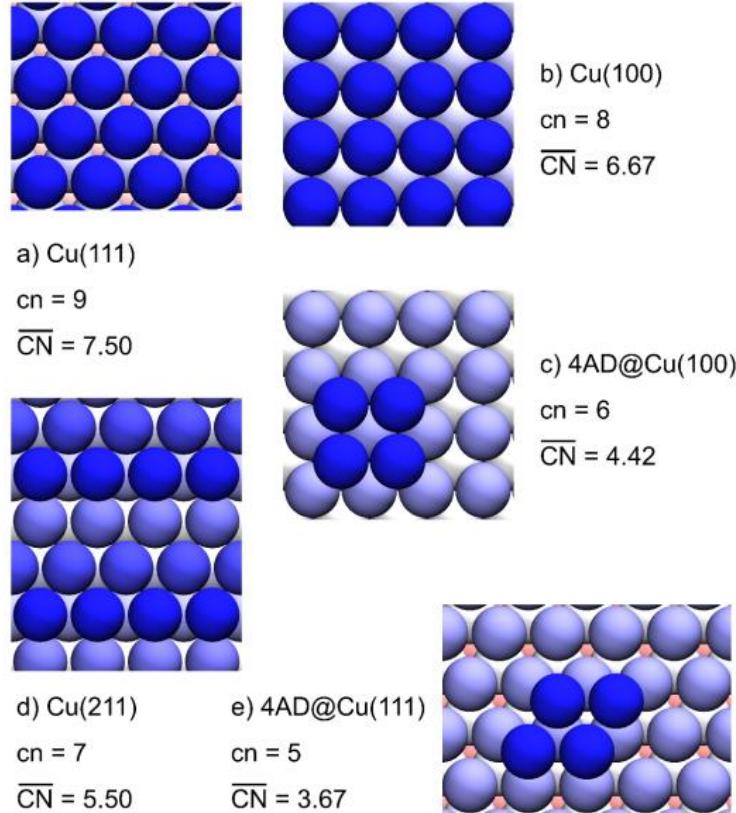
Figure S2. Top views of the five slabs under study. Different shades of blue together with white and pink colors different depths.

Conventional coordination numbers (cn) count only the first nearest neighbors of the active site "i" and assume all neighbors to be equivalent. Conversely, $\overline{CN}$ weights every neighbor "j" by their respective coordination number ($cn(j)$). Both $\overline{CN}$ and cn span the range of 0-12, because the factor cn_{max} corresponds to the maximum number of first nearest neighbors in the bulk. Hence, for atop sites $cn_{max} = 12$. $\overline{CN}$ was calculated for the five sites in this study by means of Equation S5 and the coordination number matrix in Table S5. For example for 4AD@Cu(111) we have: $\overline{CN} = \frac{(6 \times 2 + 10 \times 2 + 12 \times 1)}{12} = 3.67$.

Table S5. Coordination number matrix for the five Cu sites under study.

Site/coordination	3	4	5	6	7	8	9	10	11	12	cn	$\overline{CN}$
Cu(111)	0	0	0	0	0	0	6	0	0	3	9	7.50
Cu(100)	0	0	0	0	0	4	0	0	0	4	8	6.67
Cu(211)	0	0	0	0	2	0	9	1	0	2	7	5.50
4AD@Cu(100)	0	0	0	2	0	0	1	2	0	1	6	4.42

6

4AD@Cu(111)	0	0	0	2	0	0	0	2	0	1	5	3.67

S6. Intermediates of the most favorable pathways

In the following, we show the intermediates of the most favorable pathways for the electroreduction of glyoxal to ethylene glycol (Figure S3) and ethanol (Figure S4).

- PLS$_1$ in Figure 3 corresponds to $*CHOHCHO + H^+ + e^- \rightarrow *CHOHCHOH$.

- PLS$_2$ corresponds to $*CHOHCHOH + H^+ + e^- \rightarrow *CHOHCH_2OH$.

- PLS$_3$ corresponds to $*CH_2CHO + H^+ + e^- \rightarrow *CH_3CHO$ (or $*CH_2CHO + H^+ + e^- \rightarrow * +CH_3CHO$ if acetaldehyde is not adsorbed, see Table S4).

- PLS$_4$ corresponds to $*CH_3CHO + H^+ + e^- \rightarrow *CH_3CH_2O$ (or $*CH_3CHO + H^+ + e^- \rightarrow *CH_3CH_2O$, see Table S4).
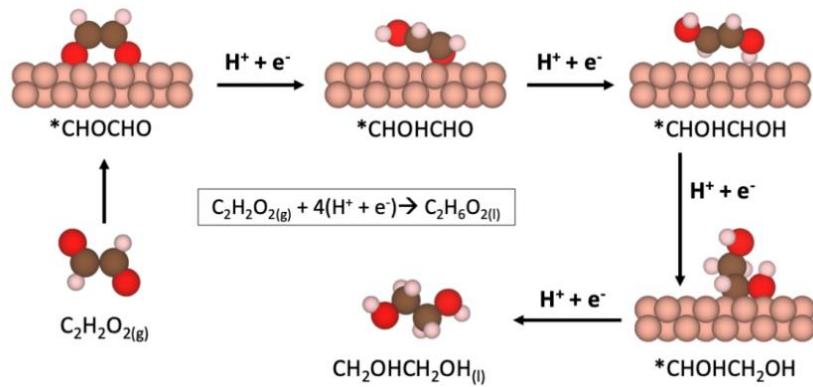
Figure S3. Most favorable electrocatalytic pathway for the GRR to ethylene glycol.
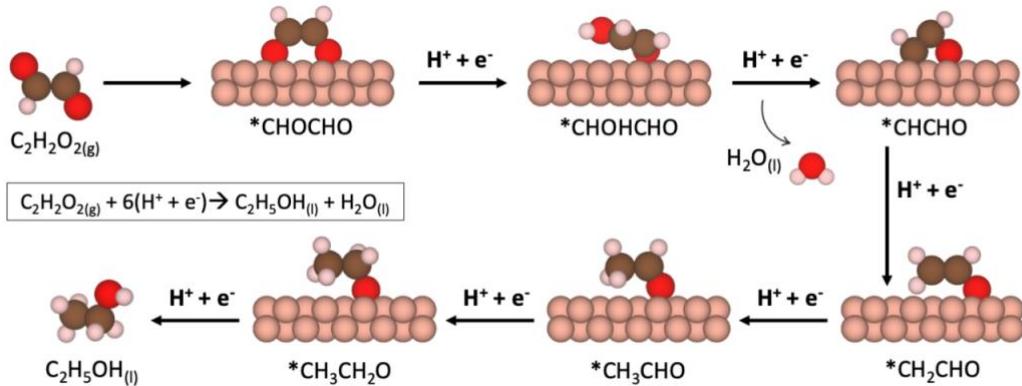
Figure S4. Most favorable electrocatalytic pathway for the GRR to ethanol.

Figures S5 and S6 show the free-energy diagrams corresponding to the pathways in Figures S3 and S4 on the five active sites under study.
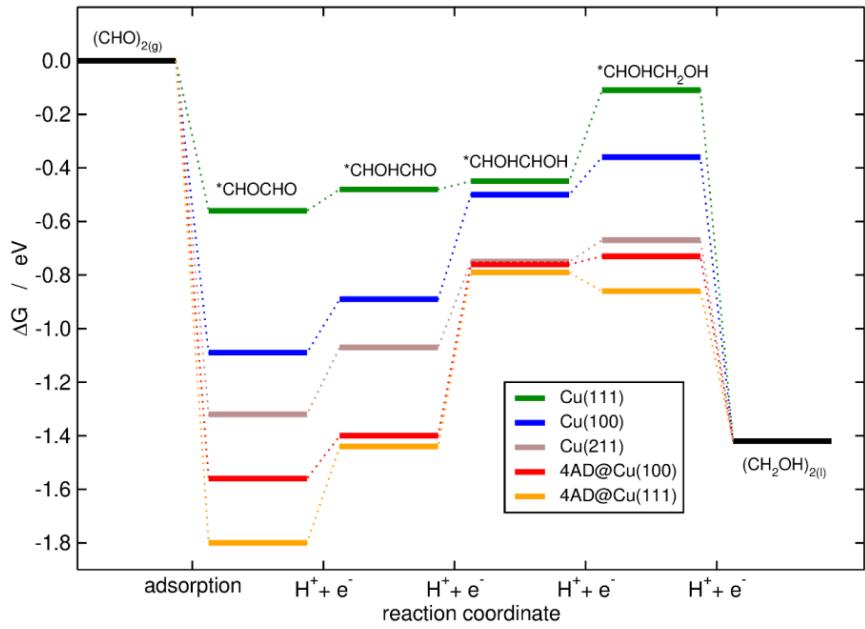
Figure S5. Free-energy diagrams at 0 V vs RHE of the most favorable pathway for glyoxal reduction to ethylene glycol on Cu(111) (green), Cu(100), Cu(211) (brown), 4AD@Cu(100) (red), and 4AD@Cu(111) (orange). The corresponding intermediates are noted for each electrochemical step. Figure S3 provides schematic views of the reaction intermediates.
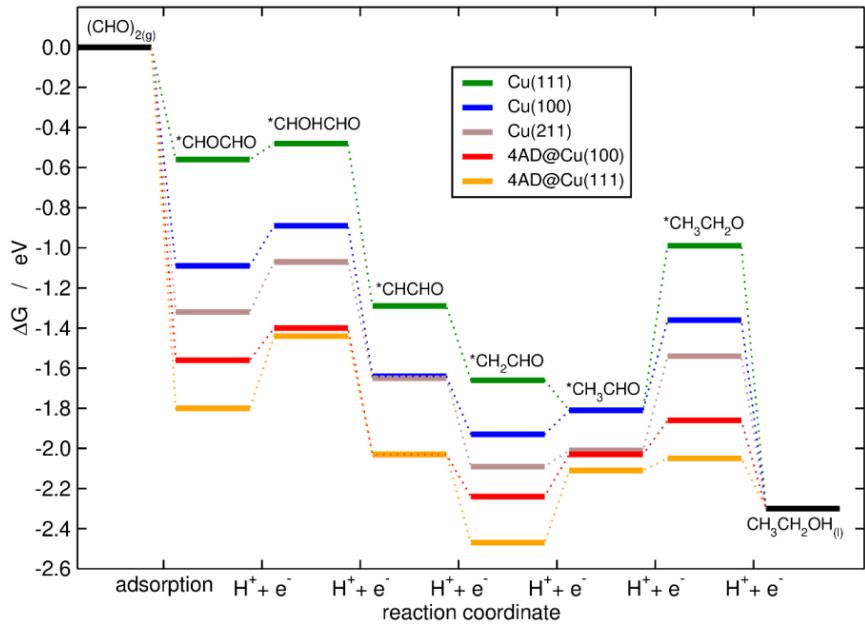
Figure S6. Free-energy diagrams at 0 V vs RHE for glyoxal reduction to ethanol on Cu(111) (green), Cu(100) (blue), Cu(211) (brown), 4AD@Cu(100) (red), and 4AD@Cu(111) (orange). The corresponding intermediates are noted for each electrochemical step. Figure S4 provides schematic views of the reaction intermediates.

S7. Optimized geometries

Here we provide the optimized geometries of the different intermediates involved in the GRR to ethylene glycol and ethanol on the five surfaces studied. For Cu(111), we also include the configuration with explicit water (in case it exists, following the iterative method in previous works).[4]

S7.1. Cu(100)

*CHOCHO on Cu(100)

*CHOHCHO on Cu(100)

*CHOCHO on Cu(100)

*CHOHCHOH on Cu(100)

*CHOHCH₂OH on Cu(100)

S7.2. Cu(111)

*CHOCHO on Cu(111)

Solvated *CHOCHO on Cu(111)

*CHOHCHO on Cu(111)
```
1.00000000000000
   10.2825149945573209    0.0000000000000000    0.0000000000000000
    5.1412575045250097    8.9049192068305896    0.0000000000000000
    0.0000000000000000    0.0000000000000000   22.8423223715796517
  Cu   C   O   H
  64   2   2   3
Selective dynamics
Direct
```

Solvated *CHOHCHO on Cu(111)
```
1.00000000000000
   10.2825149945573209    0.0000000000000000    0.0000000000000000
    5.1412575045250097    8.9049192068305896    0.0000000000000000
    0.0000000000000000    0.0000000000000000   22.8423223715796517
  Cu   C   O   H
  64   2   5   9
Selective dynamics
Direct
```

*CHCHO on Cu(111)
```
1.00000000000000
   10.2825149945573209    0.0000000000000000    0.0000000000000000
    5.1412575045250097    8.9049192068305896    0.0000000000000000
    0.0000000000000000    0.0000000000000000   22.8423223715796517
  Cu   C   O   H
  64   2   1   2
Selective dynamics
Direct
```

Solvated *CHCHO on Cu(111)
```
1.00000000000000
   10.2825149945573209    0.0000000000000000    0.0000000000000000
    5.1412575045250097    8.9049192068305896    0.0000000000000000
    0.0000000000000000    0.0000000000000000   22.8423223715796517
  Cu   C   O   H
  64   2   4   7
Selective dynamics
Direct
```

*CHOHCHOH on Cu(111)
```
1.00000000000000
   10.2825149945573209    0.0000000000000000    0.0000000000000000
    5.1412575045250097    8.9049192068305896    0.0000000000000000
    0.0000000000000000    0.0000000000000000   22.8423223715796517
  Cu   C   O   H
  64   2   2   4
Selective dynamics
Direct
```

Solvated *CHOHCHOH on Cu(111)
```
1.00000000000000
   10.2825149945573209    0.0000000000000000    0.0000000000000000
    5.1412575045250097    8.9049192068305896    0.0000000000000000
    0.0000000000000000    0.0000000000000000   22.8423223715796517
  Cu   C   O   H
  64   2   5  10
Selective dynamics
Direct
```

*CHOHCH₂OH on Cu(111)
```
1.00000000000000
   10.2825149945573209    0.0000000000000000    0.0000000000000000
    5.1412575045250097    8.9049192068305896    0.0000000000000000
    0.0000000000000000    0.0000000000000000   22.8423223715796517
  Cu   C   O   H
  64   2   2   5
Selective dynamics
Direct
```

S7.3. 4AD@Cu(100)

S7.4. 4AD@Cu(111)

S7.5. Cu(211)

*CHCHO on 4AD@Cu(111)
1.000000000000000
  10.2825516975051805   0.0000000000000000   0.0000000000000000
   5.1412758559989697   8.9049509925158592   0.0000000000000000
   0.0000000000000000   0.0000000000000000   22.8424039061621507
  Cu   C   H
  68   2   2
Selective dynamics
Direct

*CHOHCHOH on 4AD@Cu(111)
1.000000000000000
  10.2825516975051805   0.0000000000000000   0.0000000000000000
   5.1412758559989697   8.9049509925158592   0.0000000000000000
   0.0000000000000000   0.0000000000000000   22.8424039061621507
  Cu   C   O   H
  68   2   2   4
Selective dynamics
Direct

*CHOHCH₂OH on 4AD@Cu(111)
1.000000000000000
  10.2825516975051805   8.9049509925158592   0.0000000000000000
   5.1412758559989697   8.9049509925158592   0.0000000000000000
   0.0000000000000000   0.0000000000000000   22.8424039061621507
  Cu   C   O   H
  68   2   2   5
Selective dynamics
Direct

*CHOCHO on Cu(211)
1.000000000000000
   7.7167100000000000   0.0000000000000000   0.0000000000000000
   0.0000000000000000   6.3006599999999997   0.0000000000000000
   0.0000000000000000   0.0000000000000000   25.0000000000000000
  Cu   C   O
  36   2   2
Selective dynamics
Direct

*CHOHCHOH on Cu(211)
1.000000000000000
   7.7167100000000000   0.0000000000000000   0.0000000000000000
   0.0000000000000000   6.3006599999999997   0.0000000000000000
   0.0000000000000000   0.0000000000000000   25.0000000000000000
  Cu   C   O   H
  36   2   2   4
Selective dynamics
Direct

*CHOHCHOH on Cu(211)
1.000000000000000
   7.7167100000000000   0.0000000000000000   0.0000000000000000
   0.0000000000000000   6.3006599999999997   0.0000000000000000
   0.0000000000000000   0.0000000000000000   25.0000000000000000
  Cu   C   O   H
  36   2   2   4
Selective dynamics
Direct

*CHOHCHOH on Cu(211)
1.000000000000000
   7.7167100000000000   0.0000000000000000   0.0000000000000000
   0.0000000000000000   6.3006599999999997   0.0000000000000000
   0.0000000000000000   0.0000000000000000   25.0000000000000000
  Cu   C   O   H
  36   2   2   4
Selective dynamics
Direct

*CHOHCH₂OH on Cu(211)
1.000000000000000
   7.7167100000000000   0.0000000000000000   0.0000000000000000
   0.0000000000000000   6.3006599999999997   0.0000000000000000
   0.0000000000000000   0.0000000000000000   25.0000000000000000
  Cu   C   O   H
  36   2   2   5
Selective dynamics
Direct

*CHCHO on Cu(211)
1.000000000000000
   7.7167100000000000   0.0000000000000000   0.0000000000000000
   0.0000000000000000   6.3006599999999997   0.0000000000000000
   0.0000000000000000   0.0000000000000000   25.0000000000000000
  Cu   C   O   H
  36   2   2   3
Selective dynamics
Direct

References

(1)   Lide, D. R. *CRC Handbook of Chemistry and Physics*; 85th ed., CRC Press: Boca Raton, FL, USA, 2005; Vol. 268.

(2)   Granda-Marulanda, L. P.; Rendón-Calle, A.; Builes, S.; Illas, F.; Koper, M. T. M.; Calle-Vallejo, F. A Semiempirical Method to Detect and Correct DFT-Based Gas-Phase Errors and Its Application in Electrocatalysis. *ACS Catal.* **2020**, *10* (12), 6900–6907. https://doi.org/10.1021/acscatal.0c01075.

(3)   Calle-Vallejo, F.; Koper, M. T. M. Theoretical Considerations on the Electroreduction of CO to C2 Species on Cu(100) Electrodes. *Angew. Chem. Int. Ed.* **2013**, *52* (28), 7282–7285. https://doi.org/10.1002/anie.201301470.

(4)   Rendón-Calle, A.; Builes, S.; Calle-Vallejo, F. Substantial Improvement of Electrocatalytic Predictions by Systematic Assessment of Solvent Effects on Adsorption Energies. *Appl. Catal. B* **2020**, *276*, 119147. https://doi.org/10.1016/j.apcatb.2020.119147.

(5)   Pique, O.; Vines, F.; Illas, F.; Calle-Vallejo, F. Elucidating the Structure of Ethanol-Producing Active Sites at Oxide-Derived Cu Electrocatalysts. *ACS Catal.* **2020**, *10* (18), 10488–10494. https://doi.org/10.1021/acscatal.0c01880.

(6)   Ledezma-Yanez, I.; Gallent, E. P.; Koper, M. T. M.; Calle-Vallejo, F. Structure-Sensitive Electroreduction of Acetaldehyde to Ethanol on Copper and Its Mechanistic Implications for CO and CO2 Reduction. *Catal. Today* **2016**, *262*, 90–94. https://doi.org/10.1016/j.cattod.2015.09.029.